Breaking of Chiral Symmetry and Spontaneous Rotation in a Spinor Bose-Einstein Condensate

Hiroki Saito,[1] Yuki Kawaguchi,[1] and Masahito Ueda[1,2]

[1]*Department of Physics, Tokyo Institute of Technology, Tokyo 152-8551, Japan*
[2]*ERATO, Japan Science and Technology Corporation (JST), Saitama 332-0012, Japan*

(Received 11 December 2005; published 15 February 2006)

We show that a spin-1 Bose-Einstein condensate with ferromagnetic interactions spontaneously generates a topological spin texture, in which the $m = \pm 1$ components of the magnetic sublevels form vortices with opposite circulations. This phenomenon originates from an interplay between ferromagnetic interactions and spin conservation.

DOI: 10.1103/PhysRevLett.96.065302 PACS numbers: 67.57.Fg, 03.75.Kk, 03.75.Lm, 03.75.Mn

The Mermin-Ho texture [1] in superfluid ^{3}He describes an interesting thermodynamic equilibrium state, in which a circulation remains nonvanishing in a cylindrically symmetric vessel, despite the vessel being at rest. This phenomenon is due to the fact that the boundary condition at the surface of the vessel imposes a topological constraint on the $\boldsymbol{l}$ vector. In this Letter, we show that the spontaneous formation of such a topological spin texture also occurs in a Bose-Einstein condensate (BEC) of atomic gases with spin degrees of freedom [2–4].

Topological spin structures in a spinor BEC have been realized by Leanhardt *et al.* [5] using a phase imprinting technique, and the stability of such coreless vortices has been studied [6–8]. Recently, it was predicted [9,10] that the dipolar interaction also creates a coreless vortex state through a mechanism similar to the Einstein–de Haas effect.

In contrast to the Mermin-Ho texture in ^{3}He, the physical origin of the spin texture formation proposed in this Letter is the interplay between ferromagnetic interactions and spin conservation. Consider a spin-1 BEC with ferromagnetic interactions in an $m = 0$ magnetic sublevel. The spin-exchange collisions between the atoms transfer the $m = 0$ population into $m = \pm 1$ ones via $0 + 0 \rightarrow 1 + (-1)$. As a consequence, magnetization in the x-y plane may arise due to the ferromagnetic nature of the interaction. However, uniform magnetization of the entire system is prohibited because of spin conservation, which results in various spin textures [11–13]. In this Letter, we show that the topological spin texture is spontaneously generated through spin-exchange dynamics under spin conservation, where the $m = \pm 1$ components have vortices with opposite circulations. It follows from the symmetry of the Hamiltonian that there are two degenerate textures: the $m = 1$ and -1 components have $+$ and $-$ vortices, or $-$ and $+$ vortices. We show that the symmetry between these two textures is spontaneously broken in the course of the dynamics even when the initial state possesses chiral symmetry.

We consider a system of spin-1 Bose atoms with mass M confined in a potential V. The Hamiltonian of the system is given by [3,4]

$$\hat{H} = \int d\boldsymbol{r}\Big[\sum_m \hat{\psi}_m^\dagger H_0 \hat{\psi}_m + \sum_{m_{1,2,3,4}} \hat{\psi}_{m_1}^\dagger \hat{\psi}_{m_2}^\dagger \Big(\frac{g_0}{2}\delta_{m_1 m_4}\delta_{m_2 m_3} + \frac{g_1}{2}\boldsymbol{F}_{m_1 m_4}\cdot\boldsymbol{F}_{m_2 m_3}\Big)\hat{\psi}_{m_3}\hat{\psi}_{m_4}\Big], \quad (1)$$

where $\hat{\psi}_m$ is the field operator of the atom in the magnetic sublevel $m = 0, \pm 1$, $H_0 = -\hbar^2\nabla^2/(2M) + V$, and $\boldsymbol{F}$ is the spin-1 matrix. The spin-independent and spin-dependent interactions are characterized by $g_0 = 4\pi\hbar^2(a_0 + 2a_2)/(3M)$ and $g_1 = 4\pi\hbar^2(a_2 - a_0)/(3M)$, respectively, where a_S is the s-wave scattering length for the scattering channel with total spin S. In the case of spin-1 ^{87}Rb, g_1 is negative and the ground state is ferromagnetic [4,14].

When the potential V is axisymmetric with respect to the z axis, the Hamiltonian (1) is invariant under spatial reflection with respect to an arbitrary plane containing the z axis, e.g., $(x, y) \rightarrow (-x, y)$. This transformation changes a clockwise vortex $\propto e^{-i\phi}$ into a counterclockwise vortex $\propto e^{i\phi}$ with azimuthal angle ϕ. Hence, if only one of them is realized spontaneously, we call it chiral symmetry breaking. From the symmetry of the Hamiltonian, the total spin vector and the z component of the orbital angular momentum are conserved.

We consider the case in which the initial state is in the $m = 0$ mean-field ground state satisfying

$$(H_0 + g_0|\Psi_0|^2)\Psi_0 = \mu_0\Psi_0. \quad (2)$$

If the $m = \pm 1$ components are exactly zero, Ψ_0 is a stationary state of the multicomponent Gross-Pitaevskii (GP) equations,

$$i\hbar\frac{\partial\psi_0}{\partial t} = (H_0 + g_0 n)\psi_0 + \frac{g_1}{\sqrt{2}}(F_+\psi_1 + F_-\psi_{-1}), \quad (3a)$$

$$i\hbar\frac{\partial\psi_{\pm 1}}{\partial t} = (H_0 + g_0 n)\psi_{\pm 1} + g_1\Big(\frac{1}{\sqrt{2}}F_\mp\psi_0 \pm F_z\psi_{\pm 1}\Big), \quad (3b)$$

where ψ_m is the macroscopic wave function, $n = \sum_m|\psi_m|^2$, $F_z = |\psi_1|^2 - |\psi_{-1}|^2$, and $F_+ = F_-^* = \sqrt{2}(\psi_1^*\psi_0 + \psi_0^*\psi_{-1})$. The stability against excitations in the $m = \pm 1$

components is analyzed by the Bogoliubov–de Gennes equations:

$$[H_0 - \mu_0 + (g_0 + g_1)|\Psi_0|^2]u_{\pm 1}^{(\ell)} + g_1\Psi_0^2 v_{\mp 1}^{(\ell)*} = \varepsilon^{(\ell)} u_{\pm 1}^{(\ell)}, \tag{4a}$$

$$[H_0 - \mu_0 + (g_0 + g_1)|\Psi_0|^2]v_{\mp 1}^{(\ell)*} + g_1\Psi_0^{*2} u_{\pm 1}^{(\ell)} = -\varepsilon^{(\ell)} v_{\mp 1}^{(\ell)*}, \tag{4b}$$

where $u_m^{(\ell)}$ and $v_m^{(\ell)}$ are the eigenfunctions for a Bogoliubov mode with eigenenergy $\varepsilon^{(\ell)}$. From the axisymmetry of the system, the Bogoliubov modes can be classified according to the angular momentum ℓ, for which $u_m^{(\ell)} \propto e^{i\ell\phi}$ and $v_m^{(\ell)} \propto e^{-i\ell\phi}$. We find that $u_1^{(\ell)}$ couples with $v_{-1}^{(\ell)*}$ in Eq. (4), and hence the excitation of the $m = 1$ component with vorticity ℓ is accompanied by the $m = -1$ component with vorticity $-\ell$, as a consequence of the orbital angular-momentum conservation. If all the eigenenergies are real, the state Ψ_0 is dynamically stable. If there exist complex eigenenergies, the corresponding modes grow exponentially and the state Ψ_0 is dynamically unstable.

For simplicity, we restrict ourselves to two-dimensional (2D) space. This situation can be realized by a tight pancake-shaped potential $V = M\omega^2(x^2 + y^2 + \lambda^2 z^2)/2$ with $\lambda \gg 1$, where the axial confinement energy is so large that the dynamics in the z direction are frozen. In this case, the interaction strengths can be characterized by the dimensionless parameters [15] $g_j^{2D} = g_j[\lambda/(2\pi)]^{1/2}N/(a_{\rm ho}^3\hbar\omega)$, where N is the number of atoms, $a_{\rm ho} = [\hbar/(M\omega)]^{1/2}$, and $j = 1, 2$.

We numerically solve Eq. (2) by the imaginary-time propagation method and diagonalize Eq. (4) to obtain the Bogoliubov spectrum for the state Ψ_0. Figure 1 shows the lowest Bogoliubov energies for $\ell = 0$ and ± 1 as a function of g_1^{2D}, where g_0^{2D} is determined by $g_0^{2D}/g_1^{2D} = g_0/g_1 \simeq -216.1$, which is the ratio for spin-1 ^{87}Rb [16]. In the parameter regime shown in Fig. 1, the three modes exhibit complex eigenenergies. A crucial observation is that there is a region ($-3.9 \gtrsim g_1^{2D} \gtrsim -10.7$) in which only $\varepsilon^{(\pm 1)}$ are imaginary. This indicates that only these two modes are dynamically unstable in this region, where one mode has vortices $\propto e^{\pm i\phi}$ and the other mode has vortices $\propto e^{\mp i\phi}$ in the $m = \pm 1$ components. These two modes are degenerate because of the chiral symmetry of the system. In this region, we expect that the $m = \pm 1$ components start to rotate, despite there being no external rotating drive applied to the system.

In order to confirm the spontaneous rotation phenomenon predicted above, we numerically solve the GP Eq. (3) in 2D using the Crank-Nicolson scheme. The interaction strengths are taken to be $g_0^{2D} = 2200$ and $g_1^{2D} = -10.18$, with the ratio g_0^{2D}/g_1^{2D} again chosen to be that of spin-1 ^{87}Rb. For this set of interaction parameters, $\mathrm{Im}\varepsilon^{(\pm 1)}/(\hbar\omega) = 0.0707$ and all the other Bogoliubov energies are real. The initial state is the ground state of Eq. (2) for the $m = 0$ component plus a small amount of random noise in the $m = -1$ component. To extract the Bogoliubov excitations from $\psi_m(t)$, we define [17]

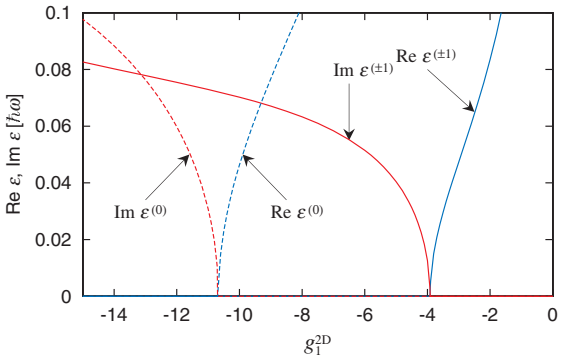

FIG. 1 (color). Real and imaginary parts of the lowest Bogoliubov energies $\varepsilon^{(\ell)}$ for $\ell = 0, \pm 1$, where the $m = \pm 1$ components of the eigenfunction are proportional to $e^{\pm i\ell\phi}$. The two energies $\varepsilon^{(\pm 1)}$ are degenerate due to the axisymmetry of the system. We have taken the parameters of spin-1 ^{87}Rb atoms, where the spin-independent interaction strength g_0^{2D} is related to the spin-dependent strength g_1^{2D} by $g_0^{2D} = -216.1 g_1^{2D}$.

$$P_{\pm 1} \equiv \left| \int d\boldsymbol{r}[e^{i\mu_0 t/\hbar} u_1^{(\mp 1)}\psi_1(t) - e^{-i\mu_0 t/\hbar} v_{-1}^{(\mp 1)}\psi_{-1}^*(t)] \right|^2, \tag{5}$$

which represents the degree of excitation in the modes $u_1^{(\pm 1)} \propto v_{-1}^{(\pm 1)*} \propto e^{\pm i\phi}$. Figure 2 shows the time evolution of $P_{\pm 1}$ and the density-phase profile of each component at $\omega t = 130$. We find that $P_{\pm 1}$ grow according to $\exp(2\,\mathrm{Im}\varepsilon^{(\pm 1)}t/\hbar)$, with their initial ratio $P_{-1}/P_1 \simeq 7.5$ kept constant, resulting in exponential growths in the angular momenta of the $m = \pm 1$ components. Thus, the $m = \pm 1$ components spontaneously rotate if the initial noise has angular-momentum fluctuations.

We consider an initial state of the system in which the chiral symmetry is preserved to great accuracy, say, $P_{-1}/P_1 = 1.0002$. The result in Fig. 2 indicates that vortices will not be created as long as the linear stability analysis is applicable. For a longer time scale, however, the chiral symmetry is spontaneously broken due to a nonlinear effect. Figure 3(a) shows the time evolution of $n_{-1} = \int d\boldsymbol{r}|\psi_{-1}|^2/N$ and the orbital angular momentum per particle $L_{-1} = -i\int d\boldsymbol{r}\psi_{-1}^*\partial_\phi\psi_{-1}/(Nn_{-1})$ for the $m = -1$ component. The $m = 1$ component is given by $n_1 \simeq n_{-1}$ and $L_1 \simeq -L_{-1}$ from spin and orbital angular-momentum conservation. The initial value for the $m = -1$ component is taken to be $\psi_{-1} = 10^{-4}r(e^{i\phi} + 1.0001e^{-i\phi})\Psi_0$, which gives $P_{-1}/P_1 \simeq 1.0002$. As long as this ratio is kept constant, the formation of the vortex states shown in the insets of Fig. 2 is not expected. In fact, as shown in Fig. 3(b), no vortex is created around the first peak of n_{-1} at $\omega t \simeq 100$. However, at $\omega t \simeq 160$, L_{-1} starts to deviate from 0 (solid blue curve) and the chiral symme-

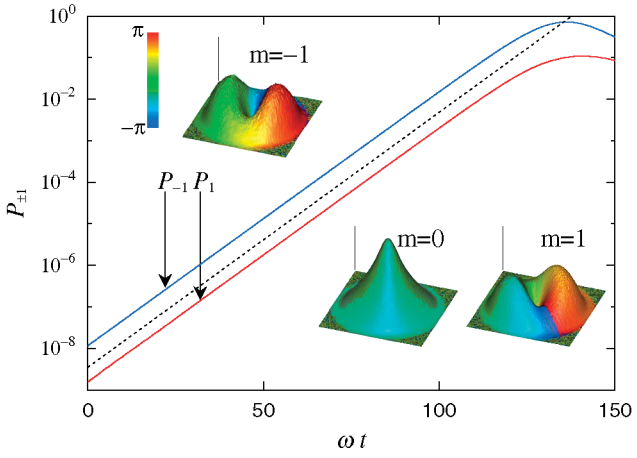

FIG. 2 (color). Degree of Bogoliubov excitation $P_{\pm1}$ in Eq. (5). The interaction strengths are $g_0^{2D} = 2200$ and $g_1^{2D} = -10.18$. The initial state is the ground state Ψ_0 of Eq. (2) for the $m = 0$ component plus a small amount of random noise in the $m = -1$ component. The dashed line is proportional to $e^{0.141\omega t}$. The insets show the density-phase profiles at $\omega t = 130$, where the size of the frame is 16×16 in units of $a_{\rm ho} = [\hbar/(M\omega)]^{1/2}$. The heights of the vertical lines in the insets indicate $|\psi_m|^2 a_{\rm ho}^2/N$, which is 0.001 for $m = \pm1$ and 0.0025 for $m = 0$.

try is dynamically broken. Consequently, the vortex states emerge in the $m = \pm1$ components as shown in Fig. 3(c).

The instability in the state with chiral symmetry [Fig. 3(b)] against forming the rotating state [Fig. 3(c)] implies that the energy of the latter is lower than that of the former. In order to confirm this, we take energy dissipation into account by replacing i on the left-hand side of Eq. (3) with $i - \gamma$ [18]. The time evolution with $\gamma = 0.03$ [19] is shown by the red curves in Fig. 3(a) and clearly indicates that the energy of the rotating state [Fig. 3(d)] is lower than that of the state having chiral symmetry [Fig. 3(b)]. For $\gamma = 0$, L_{-1} oscillates with a large amplitude due to the excess energy released from the initial state, while for $\gamma = 0.03$, the sign of the angular momentum is unchanged.

The bottom panels in Figs. 3(b)–3(d) show the spin vector distributions. In Fig. 3(b), the magnetic domains in the opposite spin directions are separated by a domain wall at $x = 0$. On the other hand, topological spin structures are formed in Figs. 3(c) and 3(d). The underlying physics of the spin structure formation is the interplay between the ferromagnetic interaction and spin conservation. The growth in the spin vectors must be accompanied by spatial spin structure formation due to the conservation of the total spin angular momentum. It should be noted that the area in which the length of the spin vector is long is larger in Figs. 3(c) and 3(d) than in Fig. 3(b), since the spin vectors must vanish at the domain wall in the latter. This is why the energy of the state in Fig. 3(d) is lower than that of Fig. 3(b). That is, the formation of the topological spin structure gains more (negative) ferromagnetic energy than the formation of the domain structure.

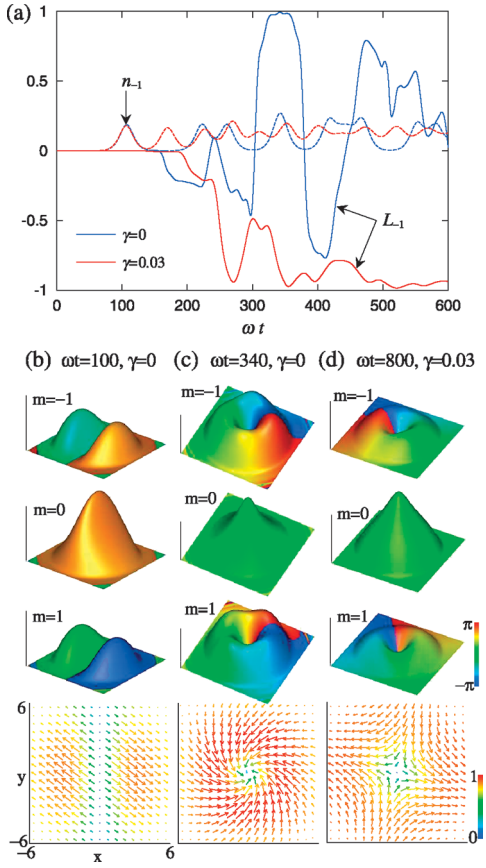

FIG. 3 (color). (a) Time evolution of the fraction n_{-1} (dashed curves) and the orbital angular momentum per particle L_{-1} (solid curves) in the $m = -1$ component with ($\gamma = 0.03$, red curves) and without ($\gamma = 0$, blue curves) dissipation. The interaction strengths are the same as in Fig. 2. The initial state is given by $\psi_0 = \Psi_0$, $\psi_{-1} = 10^{-4} r(e^{i\phi} + 1.0001e^{-i\phi})\Psi_0$, and $\psi_1 = 0$, where Ψ_0 is the ground state solution of Eq. (2). (b)–(d) Snapshots of the density-phase profiles and spin textures. The heights of the vertical lines in the density-phase profiles show $|\psi_m|^2 a_{\rm ho}/N$, which is 0.001 for $m = \pm1$ and 0.0025 for $m = 0$. The length of the vector in the bottom panels is proportional to $(F_x^2 + F_y^2)^{1/2}$ and the color represents $(F_x^2 + F_y^2)^{1/2}/(|\psi_{-1}|^2 + |\psi_0|^2 + |\psi_1|^2)$. The size of the frame is 16×16 for the density-phase profiles and 12×12 for the spin textures in units of $a_{\rm ho}$.

The above energy argument concerning the spin domain and topological structures can be reinforced by applying the variational method. We assume a variational wave function to be

$$\begin{pmatrix} 0 \\ \tilde{\Psi}_0 \\ 0 \end{pmatrix} + c\cos\theta \begin{pmatrix} u_1^{(1)} \\ 0 \\ e^{i\chi} v_{-1}^{(1)} \end{pmatrix} + c\sin\theta \begin{pmatrix} u_1^{(-1)} \\ 0 \\ e^{i\chi'} v_{-1}^{(-1)} \end{pmatrix}, \quad (6)$$

where $\tilde{\Psi}_0 = (|\Psi_0|^2 - |\psi_1|^2 - |\psi_{-1}|^2)^{1/2}$ so that the total density n is kept to be $|\Psi_0|^2$ irrespective of the values of the variational parameters, reflecting the fact that the spin-exchange process hardly changes the total density because $g_0 \gg |g_1|$ for spin-1 ^{87}Rb atoms. We minimize the energy of the system calculated from Eq. (6) with respect to c, χ,

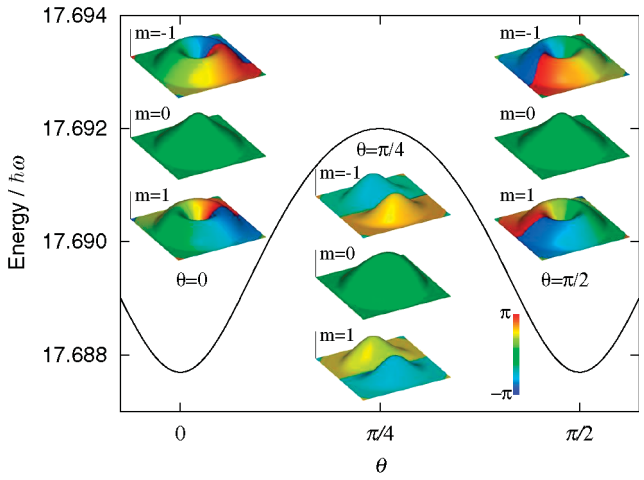

FIG. 4 (color). Energy and density-phase profiles obtained by the variational method with Eq. (6). The interaction strengths are the same as in Fig. 2. The size of the frame of the insets is 16×16 in units of $a_{\rm ho}$ and the heights of the vertical lines show $|\psi_m|^2 a_{\rm ho}^2/N$, which is 0.0005 for $m = \pm 1$ and 0.0025 for $m = 0$.

and χ' for a given θ, as shown in Fig. 4. The state at $\theta = \pi/4$, which is similar to the state shown in Fig. 3(b), has a maximum energy, while the topological spin states at $\theta = 0$ and $\pi/2$ have minimum energy, in agreement with the above discussion.

The results presented above can be realized using current experimental setups. For example, when the radial and axial trapping frequencies are $\omega = 100 \times 2\pi$ Hz and $\omega_z = 100\omega$, respectively, the interaction parameters for Figs. 2–4 correspond to $N \simeq 8880$ spin-1 ^{87}Rb atoms. The time scale for the appearance of the topological spin structure (e.g., $\omega t \sim 300$ for the initial condition in Fig. 3) is $\sim$0.5 s. If the ratio $|g_1/g_0|$ can be increased by decreasing g_0 using a Feshbach resonance or by using other atomic species, we can decrease the time scale, e.g., to about $1/10$ for $|g_1/g_0| = 1$.

In the presence of an external magnetic field B, the linear and quadratic Zeeman terms enter the Hamiltonian (1). Since the total spin is conserved, the linear Zeeman term only rotates the spin at the Larmor frequency and does not affect the dynamics. When the magnetic field is applied in the z direction, the quadratic Zeeman effect raises the energy of the $m = \pm 1$ components relative to that of the $m = 0$ component. If the quadratic Zeeman energy exceeds the ferromagnetic energy, the $m = 0$ state becomes the ground state and no excitation to the $m = \pm 1$ components occurs, which is the case for $B \gtrsim 400$ mG with $\omega = 100 \times 2\pi$ Hz, $\omega/\omega_z = 0.01$, and $N \simeq 8880$. We have numerically confirmed that the dynamics in Figs. 2 and 3 are qualitatively unchanged for a magnetic field of $\simeq 100$ mG.

In conclusion, we have proposed a novel mechanism of spontaneous formation of a topological spin structure in the spin-1 BEC prepared in the $m = 0$ state. The $m = \pm 1$ components increase exponentially from initial random seeds due to dynamical instabilities and form singly quantized vortex states (Fig. 2). Even if the clockwise and counterclockwise rotation components are assumed to be equal in an initial seed, one of them eventually becomes dominant (Fig. 3). This chiral symmetry breaking is attributed to the fact that the topological spin structure is energetically the most favorable due to the ferromagnetic interaction. This spontaneous spin structure formation is essentially caused by the spin-exchange dynamics under the constraint of spin conservation. We expect that many more interesting spin textures may also be spontaneously generated in isolated spinor BECs.

This work was supported by Grant-in-Aids for Scientific Research (Grants No. 17740263, No. 17071005, and No. 15340129) and by a 21st Century COE program at Tokyo Tech "Nanometer-Scale Quantum Physics," from the Ministry of Education, Culture, Sports, Science and Technology of Japan. Y. K. acknowledges support by the Japan Society for Promotion of Science (Project No. 16-0648). M. U. acknowledges support by a CREST program of the JST.

[1] N. D. Mermin and T.-L. Ho, Phys. Rev. Lett. **36**, 594 (1976).
[2] D. M. Stamper-Kurn *et al.*, Phys. Rev. Lett. **80**, 2027 (1998).
[3] T. Ohmi and K. Machida, J. Phys. Soc. Jpn. **67**, 1822 (1998).
[4] T.-L. Ho, Phys. Rev. Lett. **81**, 742 (1998).
[5] A. E. Leanhardt *et al.*, Phys. Rev. Lett. **90**, 140403 (2003).
[6] U. Al Khawaja and H. T. C. Stoof, Nature (London) **411**, 918 (2001).
[7] T. Mizushima, K. Machida, and T. Kita, Phys. Rev. Lett. **89**, 030401 (2002).
[8] C. M. Savage and J. Ruostekoski, Phys. Rev. Lett. **91**, 010403 (2003).
[9] L. Santos and T. Pfau, cond-mat/0510634.
[10] Y. Kawaguchi, H. Saito, and M. Ueda, cond-mat/0511052 [Phys. Rev. Lett. (to be published)].
[11] H. Saito and M. Ueda, Phys. Rev. A **72**, 023610 (2005).
[12] W. Zhang *et al.*, Phys. Rev. Lett. **95**, 180403 (2005).
[13] J. Mur-Petit *et al.*, cond-mat/0507521 [Phys. Rev. A (to be published)].
[14] N. N. Klausen, J. L. Bohn, and C. H. Greene, Phys. Rev. A **64**, 053602 (2001).
[15] Y. Castin and R. Dum, Eur. Phys. J. D **7**, 399 (1999).
[16] E. G. M. van Kempen *et al.*, Phys. Rev. Lett. **88**, 093201 (2002).
[17] Y. Kawaguchi and T. Ohmi, Phys. Rev. A **70**, 043610 (2004).
[18] M. Tsubota, K. Kasamatsu, and M. Ueda, Phys. Rev. A **65**, 023603 (2002).
[19] S. Choi, S. A. Morgan, and K. Burnett, Phys. Rev. A **57**, 4057 (1998).